



Politecnico di Torino

Porto Institutional Repository

[Article] Experimental Investigation of Nonlinear Interference Accumulation in Uncompensated Links

Original Citation:

Gabriella Bosco;Roberto Cigliutti;Antonino Nespola;Andrea Carena;Vittorio Curri;Fabrizio Forghieri;Yoshinori Yamamoto;Takashi Sasaki;Yanchao Jiang;Pierluigi Poggiolini (2012). *Experimental Investigation of Nonlinear Interference Accumulation in Uncompensated Links*. In: [IEEE PHOTONICS TECHNOLOGY LETTERS](#), vol. 24 n. 14, pp. 1230-1232. - ISSN 1041-1135

Availability:

This version is available at : <http://porto.polito.it/2497912/> since: June 2012

Publisher:

IEEE (Institute of Electrical and Electronics Engineers)

Published version:

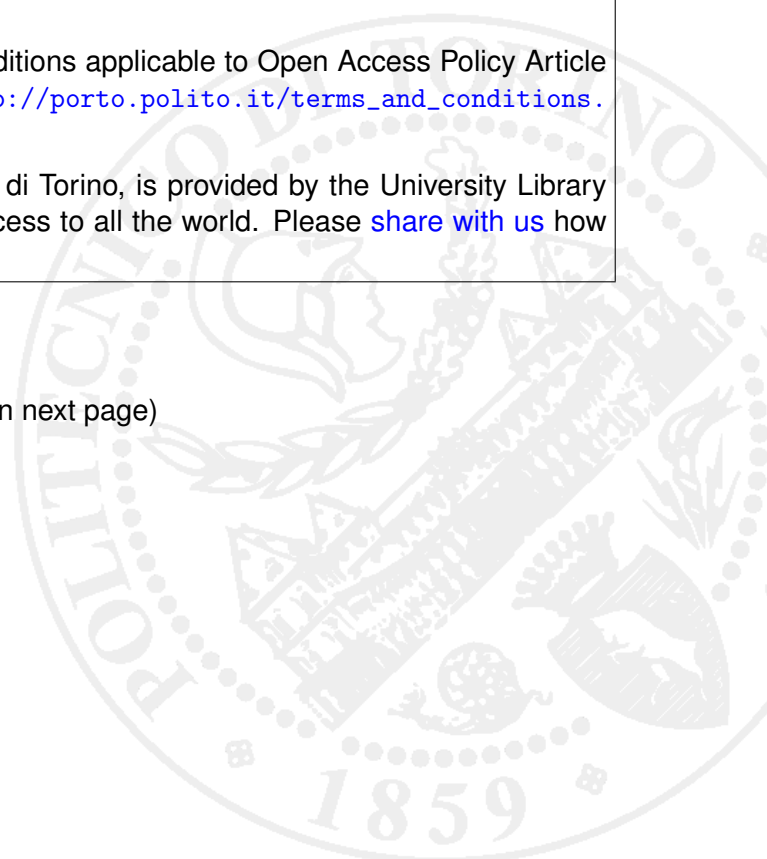
DOI:[10.1109/LPT.2012.2200672](https://doi.org/10.1109/LPT.2012.2200672)

Terms of use:

This article is made available under terms and conditions applicable to Open Access Policy Article ("Public - All rights reserved") , as described at http://porto.polito.it/terms_and_conditions.html

Porto, the institutional repository of the Politecnico di Torino, is provided by the University Library and the IT-Services. The aim is to enable open access to all the world. Please [share with us](#) how this access benefits you. Your story matters.

(Article begins on next page)



Experimental Investigation of Non-Linear Interference Accumulation in Uncompensated Links

G. Bosco, R. Cigliutti, A. Nespola, A. Carena, V. Curri, F. Forghieri, Y. Yamamoto, T. Sasaki, P. Poggiolini

Abstract—Noise due to non-linear effects in uncompensated links has recently been shown to be Gaussian and additive. We experimentally investigate the law governing its accumulation. Our results suggest a mild super-linear accumulation vs. number of spans, compatible with coherent accumulation models.

Index Terms—non-linear effects, NLI, uncompensated systems, fiber propagation

I. INTRODUCTION

RECENTLY it has been suggested that non-linear propagation effects in uncompensated links may give rise to an overall disturbance that can be approximated as additive Gaussian noise (AGN). In [1], computer simulations were shown in support. Convincing experimental proof was then provided in [2]. According to the AGN assumption, system performance is governed by a modified OSNR which includes both ASE and non-linear noise contributions as follows:

$$\text{OSNR}_{\text{tot}} = \frac{P_{\text{ch}}}{P_{\text{ASE}} + P_{\text{NLI}}} \quad (1)$$

where NLI stands for ‘non-linear interference’ and P_{ch} is the launched power per channel.

Various analytical approximated propagation models have been proposed, which provide formulas expressing P_{NLI} as a function of system parameters. Some of them resort to truncated Volterra series, others to a FWM-like approach applied to the WDM signal spectrum decomposed into small spectral slices, still others to different perturbative approaches. For a comprehensive bibliography see [3]. Notably, the equations predicting P_{NLI} bear substantial similarities across models. A key common feature of the models, and one that appears to have gained firm simulative and experimental validation, is that P_{NLI} is proportional to the launched power as P_{ch}^3 . Yet, no consensus has been reached on the key aspect of the growth of P_{NLI} vs. the number of spans.

Regarding this aspect, one hypothesis is that the NLI produced in one span is *incoherent*, and hence independent, of that produced in all other spans. If so, P_{NLI} would simply scale linearly as the number of spans N_{span} .

G. Bosco, R. Cigliutti, A. Carena, V. Curri and P. Poggiolini are with Dipartimento di Elettronica e Telecomunicazioni, Politecnico di Torino, Italy (poggiolini@polito.it). A. Nespola is with Istituto Superiore Mario Boella, Italy (nespola@ismb.it). F. Forghieri is with Cisco Photonics Italy srl, (fforghie@cisco.com). Y. Yamamoto and T. Sasaki are with Sumitomo Electric Industries, LTD, Japan (yamamoto-yoshinori@sei.co.jp). This work was supported by CISCO Systems within a SRA contract and by EUROFOS, a NoE funded by the EC through the 7th ICT-Framework Program. The simulator OptSim was supplied by RSoft Design Group Inc., the NMZ modulators by OCLARO, the balanced photodetectors by COMPEL.
Copyright (c) 2010 IEEE

Another hypothesis assumes some form of *coherent* interaction of the NLI generated in different spans. Closed-form expressions of coherent accumulation are not available but approximations or numerical solutions based on such models predict that P_{NLI} should accumulate super-linearly, that is:

$$P_{\text{NLI}} \approx P_{\text{NLI}}^{(1)} \cdot N_{\text{span}}^{1+\epsilon} \quad (2)$$

with $\epsilon > 0$. However, the currently available estimations of ϵ provide rather different values. In [1] and [4] ϵ was predicted to be about 0.25 for standard single-mode fiber (SMF). Numerical integration of the coherent model in [3] resulted in $\epsilon \approx 0.125$ for non-zero dispersion shifted fiber (at 50 GHz channel spacing) and lower than 0.1 for SMF. Experimental evidence from [2] found ϵ to be 0.37 for SMF. In [5], incoherent accumulation was measured for 28 GBaud transmission ($\epsilon = \pm 0.05$), independent of channel spacing, whereas strong superlinear accumulation was found at 11.56 GBaud: $\epsilon=0.2$ to 0.6, depending on channel spacing.

In summary, at present there are quite diverging hypotheses and results regarding the actual law of NLI noise accumulation along uncompensated links. In this paper we provide further experimental evidence, gathered from an ultra-long-haul 16-channel quasi-Nyquist-WDM polarization-multiplexed 16QAM system at 112 Gb/s per channel (14 GBaud), separately reported on in [6]. We then compare our results with those predicted by various laws. We find that the coherent model described in [3] might be a good candidate to describe NLI accumulation in this experiment. Further evidence is however needed to ascertain whether such model has a more general validity.

II. EXPERIMENTAL SETUP

The experimental setup is shown in Fig. 1. The transmitter (Tx) used a source consisting of 16 continuous-wave (CW) distributed feedback (DFB) lasers, spaced 14.7 GHz. The odd and even wavelengths were separately fed to two nested Mach-Zehnder modulators (NMZM). The NMZMs were driven by four electrical signals, each carrying one 14 GBaud 4-level amplitude-shift keying (ASK) signal, with $2^{15} - 1$ pseudo-random binary sequences (PRBSs). The four signals were generated using a single 23.8 GS/s digital-to-analog converter (DAC), whose output was suitably decorrelated through electrical delays ($\text{EDL}_1=76$ and $\text{EDL}_2=120$ symbols). Digital pre-filtering was used to obtain a square-root-raised-cosine spectrum, with bandwidth 7 GHz and roll-off 0.05. The NMZMs peak modulation depth was 30% on both I and Q modulator arms. Polarization-multiplexing (PM) was emulated

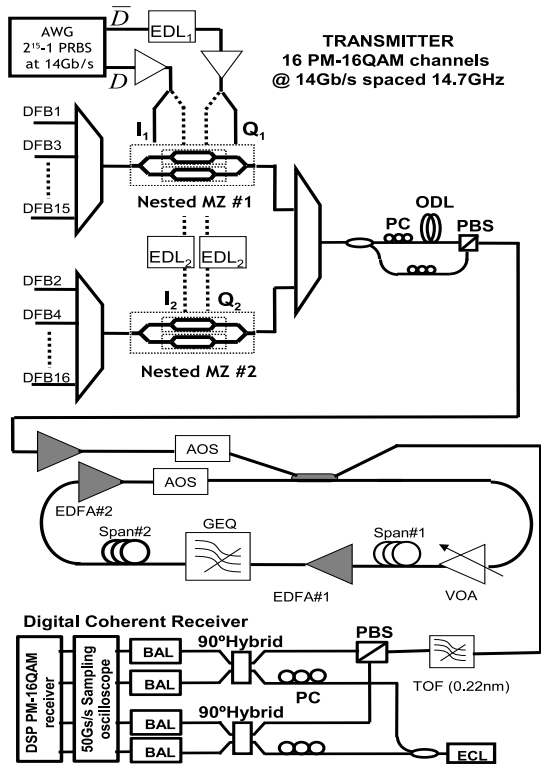


Fig. 1. The experimental set-up.

by splitting and recombining the optical signal over orthogonal polarizations, with optical decorrelation (ODL, 64m of fiber). The 16-channel signal was then launched into a re-circulating fiber loop consisting of two spans of uncompensated pure silica-core fiber (PSCF) with length 54.04 and 54.79 km. Fiber loss was 0.162 dB/km, dispersion 21 ps/nm/km and effective area $130 \mu\text{m}^2$. The loop made use of erbium-doped fiber amplifiers (EDFA) and included a gain-equalizer (GEQ). The receiver (Rx) had a standard set-up for coherent reception, with a tunable external-cavity laser (ECL) as local oscillator (LO) and a dual 90-degree hybrid followed by dual-balanced photodetectors (BAL). A 50 GS/s real-time oscilloscope was used to sample the signals. The Rx off-line digital signal processing section consisted (in order) of re-sampling to 2 samples per symbol, bulk chromatic dispersion (CD) compensation, a 43-taps butterfly stage driven by a multi-modulus CMA (constant-modulus algorithm), a Viterbi&Viterbi stage and finally maximum-likelihood decision. An ECL was used as Tx laser for the channel under test, distinct from the LO, replacing a DFB in the comb. At the Rx input, we inserted a tunable optical filter (TOF) with bandwidth 0.22 nm, to prevent excessive optical power from reaching the Rx. More details can be found in [6].

III. NON-LINEAR INTERFERENCE ESTIMATION

Fig. 2a shows the optically measured linear OSNR after each span ($\text{OSNR}_{\text{lin}} = P_{\text{ch}}/P_{\text{ASE}}$), where P_{ASE} is the noise power due both to ASE noise introduced by optical amplifiers

outside the recirculating loop and to ASE noise accumulation along the link. The measured values deviate from the expected N_{span}^{-1} dependence, which would be a straight downward line. This is due to ASE noise produced by the EDFAs outside the loop, which resulted in a measured OSNR of 30.3 dB (over 0.1 nm) at zero recirculations. When this additional ASE noise is calibrated out of the linear OSNR, a downward straight line is indeed found, shown as a dashed-dotted line in Fig. 2a. The corresponding noise figure of loop EDFAs is 5.7 dB, in good agreement with the one found through a stand-alone characterization of the EDFAs at the same operating point.

Following, we accurately measured the Tx-Rx pair BER vs. the noise-loaded back-to-back OSNR (Fig. 2b), with all channels turned on. From this characterization we derived the best-fit BER-vs.-OSNR law of the Tx-Rx pair shown in Fig. 2b, called Φ . Then, in linearity, the system BER along the link would ideally be: $\text{BER} = \Phi(\text{OSNR}_{\text{lin}})$. However, when non-linearity is present, according to Eq. (1) the OSNR accumulated along the link is due not only to P_{ASE} but also to P_{NLI} and the BER is therefore given by:

$$\text{BER} = \Phi(\text{OSNR}_{\text{tot}}) \quad (3)$$

Defining: $\text{OSNR}_{\text{NLI}} = P_{\text{ch}}/P_{\text{NLI}}$, from Eq. (1) we can write:

$$\text{OSNR}_{\text{tot}}^{-1} = \text{OSNR}_{\text{lin}}^{-1} + \text{OSNR}_{\text{NLI}}^{-1} \quad (4)$$

Then, inserting Eq. (4) into Eq. (3), taking Φ^{-1} of both sides and performing straightforward manipulations, we can finally write:

$$P_{\text{NLI}} = \left[\frac{1}{\Phi^{-1}(\text{BER})} - \frac{1}{\text{OSNR}_{\text{lin}}} \right] \cdot P_{\text{ch}} \quad (5)$$

Therefore, if BER is measured experimentally, and using OSNR_{lin} from Fig. 2a, then an estimate of P_{NLI} can be found through Eq. (5).

We measured the system BER on channel #8 (one of the two center ones) vs. N_{span} , at the optimum launch power of -6 dBm per channel. The results are shown as markers in Fig. 2c, together with the best-fit curve (dashed line). We then extrapolated the P_{NLI} values through Eq. (5), using the best-fit curves in the three plots of Fig. 2. The resulting plot of P_{NLI} vs. N_{span} is shown in Fig. 3 as markers.

We then compared the results with those predicted by the models reported in [3]. Note that, according to the nonlinear model, the scaling factor ϵ is independent of the launch power. The curve labeled ‘coherent’ was found using the coherent accumulation model of Eq. (18) in [3]. All other curves were plotted according to Eq. (2), as follows: first, $P_{\text{NLI}}^{(1)}$ was calculated using Eq. (15) in [3], yielding 16.06 [nW]. Then, the bottom curve was drawn assuming $\epsilon=0$ (incoherent accumulation), while the top three curves were drawn assuming $\epsilon = 0.2, 0.3$ and 0.4 . In addition, we found that the coherent accumulation curve too can almost perfectly be expressed through Eq. (2), with the same $P_{\text{NLI}}^{(1)}=16.06$ [nW] and $\epsilon=1.116$.

Note that Eqs. (15) and (18) in [3] require parameters that are found experimentally but are completely independent of the BER and OSNR measurements used to estimate the P_{NLI} markers in Fig. 3. Specifically, they are: fiber dispersion, non-linearity and loss coefficients, span length, channel spacing and number of channels.

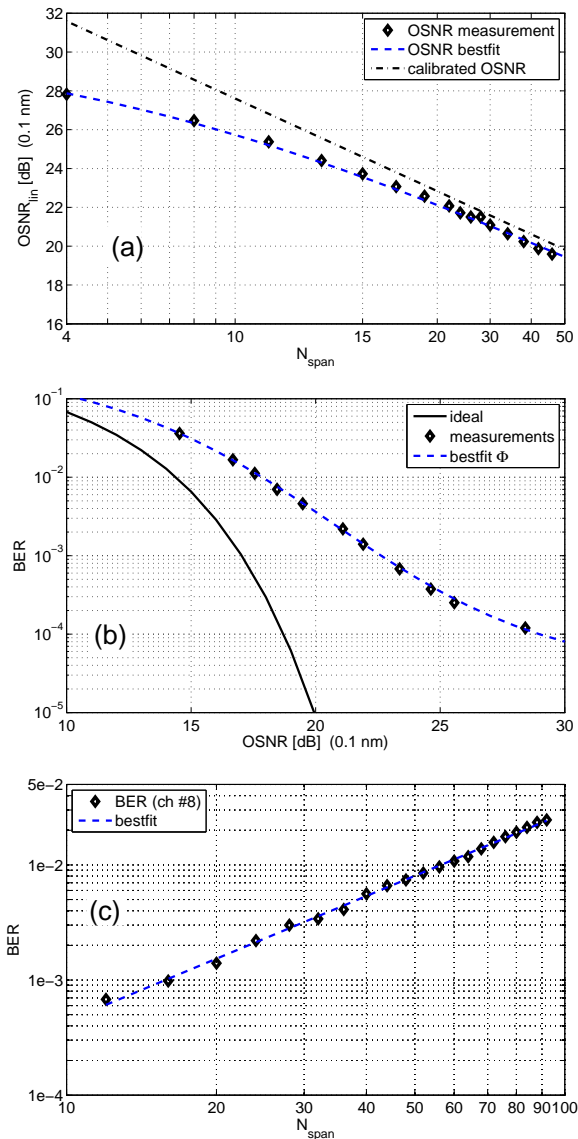


Fig. 2. (a): measured OSNR along the link vs. span number N_{span} (markers and dashed line bestfit); calibrated OSNR, due to only ASE noise accumulation in the loop (dashed-dotted line). (b): measured BER vs. calibrated OSNR (markers) in back-to-back, for channel # 8, with all channels turned on, and best-fit law Φ (dashed line). (c): measured BER vs. N_{span} (markers) and bestfit (dashed).

IV. COMMENTS AND CONCLUSION

The experimental markers and the coherent accumulation curve in Fig. 3 appear very close. This is remarkable, as they are derived in a completely different way, based on parameters found through independent measurements. This correspondence suggests that the coherent model of [3] might be a possible analytical candidate to describe NLI accumulation.

On the other hand, we must point out that the measurement of P_{NLI} accumulation is rather delicate and sensitive to errors. Assuming a possible independent error of ± 0.5 dB on all three of the key measured quantities OSNR, OSNR_{lin} and P_{ch} , the wide 90% confidence intervals shown in Fig. 3 are found. We strived to carry out accurate measurements, but errors of this extent are possible. According to the error bars,

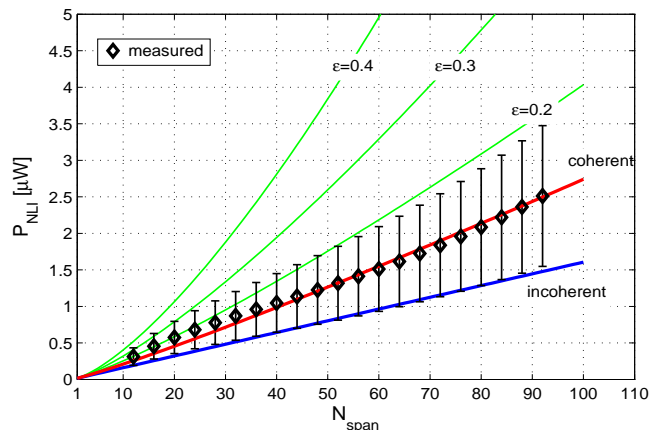


Fig. 3. Markers: measured non-linearity power P_{NLI} vs. N_{span} . Error bars: 90% confidence intervals. Solid lines, according to labels: incoherent accumulation, coherent accumulation and (three top curves) Eq. (2) with $\epsilon = 0.2, 0.3$ and 0.4 .

although at the extremes, both incoherent accumulation on the low end or super-linear accumulation with $\epsilon = 0.2$ would still be compatible, though less likely, with our results.

Instead, we believe that our results are incompatible with strong non-linear accumulation: bringing the markers close to the top two curves of Fig. 3 would require assuming unrealistically large systematic measurement errors of several dB's on the listed quantities. Therefore, at least in the context of our set-up, we believe we can rule out these larger exponents.

This does not mean that, in general, large exponents such as those found at 100G in [2] or at 40G in [5] cannot occur, depending on specific set-ups. Many models, including [3], predict that NLI accumulation does depend on various system parameters (e.g. symbol rate, number of channels, frequency spacing fiber type) although in a non-straightforward way.

In summary we believe that our results contribute to the experimental evidence regarding NLI noise accumulation in the sense of suggesting that mild super-linear accumulation, similar to the coherent accumulation model proposed in [3], could take place in actual systems. However, the problem of NLI accumulation is complex and further investigation, both theoretical and experimental, is needed to settle it.

REFERENCES

- [1] A. Carena et al., "Statistical Characterization of PM-QPSK Signals after Propagation in Uncompensated Fiber Links," in *Proc. of ECOC 2010*, Torino (Italy), paper P4.07, Sept. 2010.
- [2] F. Vacondio, et al., "On nonlinear distortions of highly dispersive optical coherent systems," *Optics Express*, vol. 20, no. 2, Jan. 2012, pp. 1022-1032.
- [3] A. Carena et al., "Modeling of the Impact of Non-Linear Propagation Effects in Uncompensated Optical Coherent Transmission Links," *J. Lightw. Technol.*, vol. 30, no. 10, May. 15 2012, pp. 1524-1539.
- [4] A. Bononi, E. Grellier, P. Serena, N. Rossi, and F. Vacondio "Modeling Nonlinearity in Coherent Transmissions with Dominant Interpulse-Four-Wave-Mixing," in *Proc. of ECOC 2011*, paper We.7.B.4, Geneva (CH).
- [5] O. V. Sinkin, et al., "Scaling of Nonlinear Impairments in Dispersion-Uncompensated Long-Haul Transmission," in *Proc. of OFC 2012*, Los Angeles (US), paper OTu1A.2, Mar. 2012.
- [6] R. Cigliutti et al., "Ultra-Long-Haul Transmission of 16x112 Gb/s Spectrally-Engineered DAC-Generated Nyquist-WDM PM-16QAM Channels with 1.05x(Symbol-Rate) Frequency Spacing," in *Proc. OFC 2012*, paper OTh3A.3, Mar. 2012.